TRANSDUCER-SHAPE OPTIMIZATION FOR ANGLE ESTIMATION OF A BROADBRAND MONAURAL SONAR SYSTEM

Jonas REIJNIERS and Herbert PEREMANS

Departement Milieu, Technologie en Technologiemanagement,
Universiteit Antwerpen, Prinsstraat 13, 2000 Antwerpen

Abstract: In this paper we describe a procedure for the search of the optimal transducer geometry for a monaural, broadband sonar system. We restrict ourselves to a simple transducer morphology that can be technologically realized: a radially symmetric two-dimensional piston transducer with adaptable electrode shape. We use a genetic algorithm to obtain the `optimal' geometry, and show that the generated transducer performs significantly better in simulated localization experiments.

Keywords: artificial intelligence, bionics, computer simulation, digital signal processing, mobile robots.

1. INTRODUCTION

In this paper we elaborate on our recent work (Reijniers and Peremans, 2004) in which we investigate echolocation by spectral analysis as a possible mechanism used by bats to navigate through their natural environment (Thomas, *et al.*, 2003). We propose a method to localize natural reflectors, i.e. a large number of closely spaced scatterers, on the basis of the time-frequency representation of the returned echo that is calculated by the bat's cochlea. This method reconstructs the environment by comparing the returned echoes with predefined templates corresponding with echoes from different angles. It was shown to allow useful navigation behaviour, although it is prone to the generation of ghost images, i.e. erroneous interpretations of ambiguous position estimates.

There are two different, yet complementary approaches to reduce the occurence of ghost images. In our earlier work (Reijniers and Peremans, 2004), we concentrated on how active control of the ear configuration allows binaural sonar systems to eliminate ghost images by combining the results from a sequence of measurements, each corresponding with a well chosen ear configuration. In this paper we follow a different approach and argue that a well-chosen geometry of the emitter/receiver transducer can minimize such ambiguities. We propose the use of genetic algorithms (GA) to search for the optimal shape.

Despite the description in this paper being restricted to the two-dimensional (2D) situation, this is not essential, and we discuss how the mechanism described can be straightforwardly extended to the three-dimensional case as it occurs in nature.

2. SIMULATION MODEL

In the interest of clarity we study the simplest situation and consider a radially symmetric piston-like transducer which acts both as emitter and receiver. Consequently, the problem can be fully described using a single angle θ. First we consider a full piston transducer. Only pointlike sources radiate sound equally in all directions, sound sources of finite extent instead have a frequency dependent directivity, also called radiation pattern $H_p(\theta,f)$ (s. Fig.1). Hence, a sonar system does not emit the same call in all directions and objects situated at different bearing angles are sounded by pulses with a different frequency content. Similarly, upon reception the echoes returning from the environment undergo a second filtering caused by the finite spatial extent of the receiver.

This paper was recommended for publication by Dorel AIORDACHIOAIE

Because of reciprocity, this is exactly the same filtering as was done by the emitter (Pierce, 1994).

We consider a broadband call $S_c(f)$ of 2ms duration. The amplitude increases from zero to full strength in 0.5ms, remains constant for 1ms and then decreases again in 0.5ms. The instantaneous frequency of the call sweeps down from 100 to 20kHz. A spectrogram-like representation of this emit signal is shown in Fig. 2(a). Such call duration and frequency sweep are in accordance with experimental data on fm-bat vocalizations.

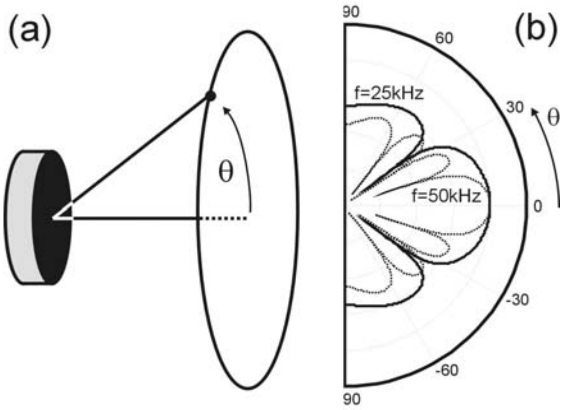

Fig. 1. (a) Radially symmetric piston transducer. (b) Radiation pattern $H_p(\theta,f)$ of a full piston transducer with diameter=3cm, for f=25kHz (solid curve) and f=50kHz (dotted curve).

For the complete echo formation process, assuming a target at position (r,θ), linear physical phenomena throughout the echo formation and denoting the call spectrum by $S_c(f)$, we can express the echo spectrum $S_f(f)$ (Peremans, 1997) as

$$(1)\quad S_e(f) = H_p(\theta,f) H_{air}(f) H_{refl}(f) H_p(\theta,f) S_c(f),$$

where for the monaural system both the transmitter and the receiver result in identical filter contributions $H_p(\theta,f)$ and the propagation of the sound pulse through the air is modeled by

$$(2)\quad H_{air}(f) = e^{-\alpha(f)2r} e^{-j2\pi f\, 2r / v_{sound}}$$

The latter expression contains propagation delay and frequency dependent absorption. Note that none of these contributions are angle dependent.

The last term $H_{refl}(f)$ to explain represents the reflection process occurring at one of the reflecting facets of the natural reflector, e.g. the leaf of a tree. In this paper we only consider pointlike reflectors, i.e., we take reflection to be due to omnidirectional and frequency independent diffraction, i.e., $H_{refl}(f)=C/r^2$, with C a constant and the term $1/r^2$ modeling the spherical spreading.

To process the incoming echo, we used a gammatone filter bank model, consisting of 77 frequency channels with central frequencies ranging between [10kHz, 150kHz] and with constant quality factor $Q=20$. Keeping filter quality constant implies that bandwidth (f_{bw}) is a linear function of center frequency (f_c): $f_{bw}=f_c/Q$. Additionally, overlap between neighbouring filters is kept constant (Slaney, 1993), which results in a wider spacing of filters as bandwidth increases. Next, the output of the filterbank is processed with a half-wave rectifier and a low-pass filter. These last two steps are equivalent to a simple amplitude demodulation scheme that approximately recovers the envelope of the outputs of the bandpass filters in the filter bank. These operations are a simple, yet effective model of the processing performed by the cochlea (Schroeder and Hall, 1974).

3. ANGULAR TEMPLATE MATCHING

As a result of the filter operations performed by the sound generation and reception apparatus of the sonar system the bearing information of a reflector is encoded in the spectrum of the echo. We now show how this property can be used to localize natural reflectors consisting of many closely spaced point scatterers.

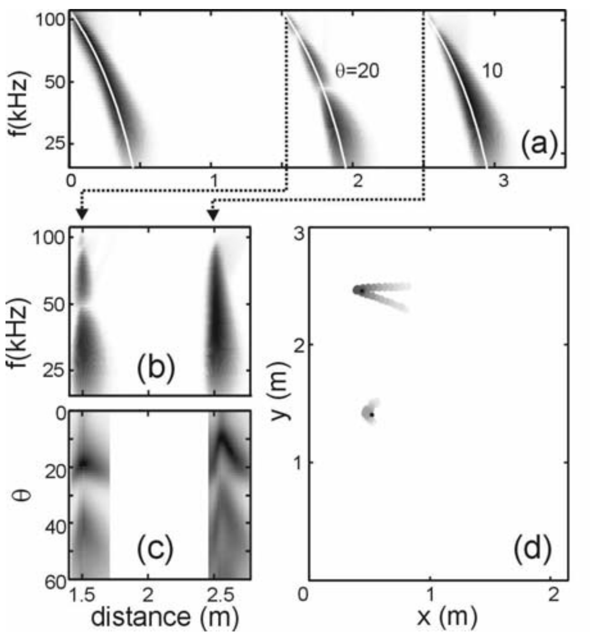

Fig. 2. (a) Cochlear time-frequency representation of picked up call + echoes from two spatially well separated reflectors (time axis rescaled into traveled distance axis). (b) Cochlear output after call induced delay variation has been compensated for. (c) The correlation function, correlation(θ,r), calculated for the cochlear output shown in (a). (d) The estimated positions (larger gray dots) and the true positions (black dots) of the reflectors.

As described above, we make use of Eq.(1) and the cochlear model to calculate the expected echo $s_e(t)$

and its corresponding cochlear response for a single pointlike reflector placed at different bearings. As echo travel time τ is related in a systematic way with distance, i.e. $\tau=2r/v_{sound}$, the distance dependencies of the echo signal can be easily compensated for by a time dependent gain compensation. All results shown below assume such compensation for distance dependencies has been applied. Next, we store the cochlear responses in a set of templates. Because of the finite response times of the cochlear frequency channels, these templates are two dimensional objects (frequency vs. time/distance) as is clear from Fig. 2 (a). However, we note that it is sufficient to consider only the maximum filter output, i.e. the values along the white curves in Fig. 2 (a), to estimate the angular information. Indeed, these maxima provide the weights applied to the known responses of the cochlear frequency channels to the call. Note that because of the frequency swept nature of the latter, the different frequency channels of the cochlea attain a maximum at different points in time. However, we assume that the received signal as processed by the cochlea also contains the call so that the systematic variation of frequency over time present in the call can be compensated for in the received echoes, see Fig. 2 (b), and a self-calibrating system results. This calibration has been applied to all the cochlear outputs shown below.

In order to build our database of angle dependent templates, we position a point reflector at every angle and calculate the corresponding cochlear output. To remove signal strength dependencies this output is normalized before storing it as a template $T_\theta(n)$, with n=1…N and N cochlear frequency channels. The resulting set of templates for the monaural sonar system is shown in Fig. 3 (b).

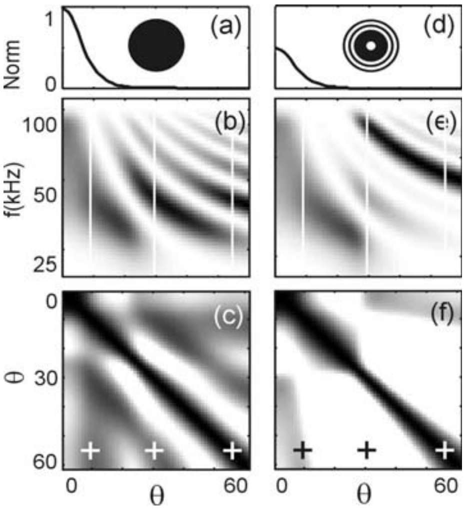

Fig. 3. Full/evolved transducer: (a/d) the norm of the templates before normalization, (b/e) the angular templates, (c/e) the correlation matrix of the angular templates. Only the fractions larger than 0.5 are shown.

We note that there is a symmetry around θ=0 which means that with this monaural system one cannot distinguish left from right. We notice that with increasing θ increasing numbers of notches are shifted in from the high frequency region.

4. MATCHING WITH TEMPLATES

4.1 Isolated echoes

Suppose we have a composite echo consisting of two echoes originating from two different point reflectors, positioned at different angles θ=10°, 20° and different distances r=1.5, 2.5m. The echo as processed by the cochlea is shown in Fig.2 (a). To reconstruct the environment we compare the normalized cochlear output pattern $S_{cochlea}(n,r)$ at every distance r with the set of angular templates, and search for the one that resembles the cochlear output the most. The echo corresponding with that particular distance r is then assumed to come from the corresponding direction.

Hence, in order to find the template $T_\theta(n)$ which is closest to the cochlear output pattern at distance r we calculate its correlation with each of the angular templates

$$Correlation(\theta, r) = \sum_{n=1}^{N} T_\theta(n) S_{cochlea}(n, r), \quad (3)$$

with N the number of cochlear frequency channels. This correlation function calculated for the cochlear output shown in Fig.2 (a) is shown in Fig.2 (c). In Fig.2 (d) we plot the estimated angle (circular dots), i.e. the angle corresponding with the maximal correlation, see Fig.2 (c), for every r. We use the total, i.e. summed over all frequency channels, power of the cochlear output at that distance r to weigh the importance of the corresponding angle estimate. Hence, we can limit angle estimation to those distances that correspond with sufficiently high cochlear output power. Every dot has a gray-value set by its associated cochlear output power: black corresponds to highest intensity, white to zero intensity. From this example we conclude that this scheme results in accurate position estimates as long as the reflectors are radially separated giving rise to isolated, i.e. non-overlapping, echoes.

4.2 Overlapping echoes

When navigating through a natural environment, e.g. foliage, the received echoes are much more complicated and composed of large numbers of overlapping echoes caused by the different reflecting facets of the natural reflectors, e.g. trees. Applying the approach outlined above to this more complex situation results in less ideal performance, as illustrated by Fig.4 (c). This performance loss can be explained by the following observations.

If we consider a more complex environment, as in Fig.4, the echoes from these reflecting facets will interfere and give rise to a cochlear output pattern that is not so straightforward to classify, see Fig.4 (a). Indeed, non-linearities in the cochlear processing make it impossible to compose such cochlear outputs out of linear combinations of the memorized templates. In a particular frequency channel of the cochlea interference occurs whenever the response time of that frequency channel is longer than the delay between two echoes. Hence, we conclude that such interference effects are most pronounced for the low frequency channels as they have the longest response times. As can be seen from Fig.4 (b) and (c) these interference effects result in a number of incorrectly positioned reflectors (ghost images). The effect is further aggravated by the non-orthogonality of the set of templates. As a result different templates corresponding with different bearing angles have similar correlation values when compared with the cochlear output, as is shown in Fig.3 (c): the regions (white crosses) indicated on the horizontal line corresponding with θ=55° have similar correlation. This problem can be minimized by choice of a sonar system which exhibits little correlation between the different angular templates.

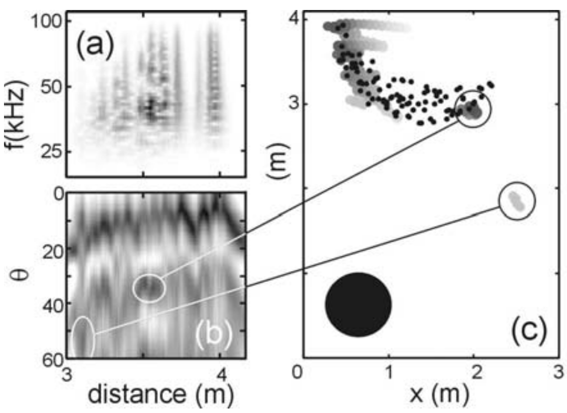

Fig. 4. (a) Cochlear output for the scene shown in (c); (b) Overlap between the templates and the cochlear output at each distance r; (c) A tree consisting of multiple pointlike reflecting facets (black dots) and their estimated positions (larger gray dots).

Also, this scheme allows detection of only one angle (reflector) for every distance r. This can be understood by noting that the strength of an echo is highly correlated with the angle, as can be inferred from Fig.3 (a) where the norm of the templates before normalization is shown. Smaller angles correspond with higher strengths, and consequently, the template matching, in the presence of interfering echoes, is predominantly driven by the strongest echo. Hence, in the presence of multiple overlapping echoes the localization mechanism described above returns preferentially the position estimates of those targets that correspond with the smallest bearing angles.

Here we try to optimize the transducer itself, by considering more complex shapes. Indeed, we conjecture that minimizing such ambiguities has been one of the driving forces in the evolution of the, often complexly shaped, bat pinnae that can be observed in nature [Fig.5 (a)].

5. OPTIMIZATION OF THE SONAR SYSTEM

In contrast to the 3D-shaped bat pinnae and noseleafs, we restrict ourselves to a simplified morphology that can be technologically realized: a radially symmetric 2D piston transducer with tunable shape. A new technology, the so-called electro-magnetic film (EMFi), permits realization of these complex transducer shapes. This EMFi behaves like a soft and sensitive piezoelectric, and can be used to interconvert acoustical and electrical signals (Bauer *et al.*, 2004). Sandwiched between two electrode surfaces, the ferroelectric film expands or shrinks when an positive/negative voltage is applied. Inversely, the ferroelectret will generate a voltage if a pressure is applied, and hence can also be used as a receiver. The shape of the transducer can be modified by changing the shape of one of the electrode surfaces, since only those parts of the ferroelectret sandwiched between two electrodes will take part in the transduction.

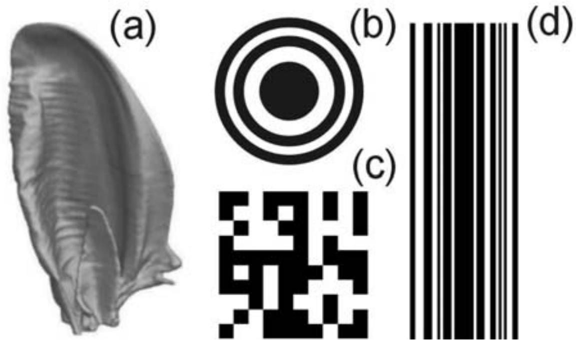

Fig. 5. (a) The pinna of the Brown long-eared bat (Bat specimen provided by the Dept. of Zoology, University of Erlangen). Evolution has equipped the bat with a complex earshape in order to perform its sonar based localization. (b), (c) and (d) are front views of different geometries of a 2D piston transducer. In this paper we only consider the radially symmetric geometry (b).

Considering a 2D transducer, different geometries are possible, as is shown in Fig.~\ref{geometries}. In this paper we will focus on transducer (b), i.e., a radially symmetric piston transducer, with variation along the r-axis. Transducers with different electrode shapes will give rise to a different radiation pattern and consequently will have different sets of angular templates. The radiation pattern can be calculated using Huygens' theorem, \cite{pierce1} and reads:

$$H_p(\theta, f) \propto \int Chrom(r) r J_0(kr \sin\theta) dr \,. \quad (4)$$

Chrom(r) is the binary representation of the radial distribution, which we use as "chromosome" in the genetic algorithm. Indeed, as this optimization is similar to the problem solved by evolution, i.e. the bat pinna shapes in nature, we use a genetic algorithm to obtain the 'optimal' transducer geometry for our purposes. Because of radial symmetry, the gene is represented as an array of N=20 bits, where 0 and 1 correspond respectively to 'not-vibrating' and 'vibrating' material. The maximum radius we set to R_{max}=1.5cm. Increasing N did not significantly change the results.
The angular templates read:

$$T_\theta(f) = \left|H_p(\theta, f)\right|^2 A(f), \quad (5)$$

where A(f) is a frequency dependent amplitude modulation as introduced by our cochlear filter [see Fig.2 (a)]. As fitness value we take:

$$fitness = \sum_{i,j} \max\left[0.5, \int T_{\theta_i}(f) T_{\theta_j}(f) df\right], \quad (6)$$

i.e., we sum over the correlation matrix, but only take into account the values larger than 0.5. We do this because we prefer all templates to differ at least slightly from each other, rather than that some have no correlation and others are almost equal.

In addition to this fitness value, we also have an energy constraint on the transducer: the total emitted energy should at least be half that of a full piston transducer. Moreover we want the spectral energy to decrease monotonically with increasing angles [as is the case for the full piston as can be seen in Fig.3 (a,d)], in order to reduce ambiguities. If several reflectors are positioned at equal distance but at different angles, those positioned at small angles will dominate the echo and consequently will be detected.

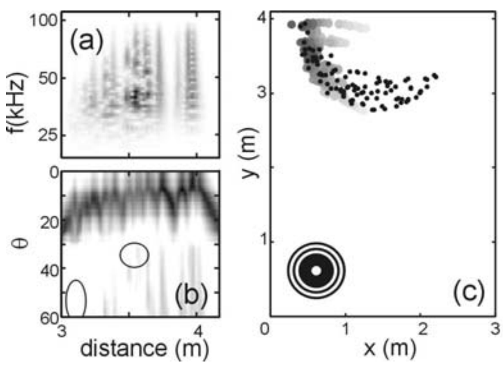

Fig. 6. The same as in Fig. 4, but now for the evolved transducer.

6. RESULTS

Using this evolutionary approach, we arrive at the transducer shown in the inset of Fig.3 (d). In Fig.3 the norm of the angular templates, the angular templates and the correlation matrix is shown respectively for the full and the optimized transducer. The norm of the templates is correlated with the energy which is emitted in different directions. From Fig.3 (f) we notice that the overall correlation, and especially the regions with high correlation between the templates (marked with white crosses) are significantly reduced. As can be seen in Fig.3 (e), this is realized by suppression of some of the sidelobes of the angular templates, such that the corresponding templates attain their maximum at different frequencies and hence have less correlation.

If we use the optimized transducer in the same experimental setup as in Fig.4, we obtain the results shown in Fig.6. Fig.6 (b) shows us that correlation is much more concentrated around one angle, and that the ghost images shown in Fig.4 are no longer present with this transducer.

7. CONCLUSIONS

In this paper we proposed a transducer shape optimization strategy to increase the performance of a monaural broadband sonar system in an angle estimation task. We concentrated on a radially symmetric 2D transducer, and used a genetic algorithm to arrive at an optimal electrode geometry. Selection happens so that the correlation between angular templates is minimal and energy decays continuously with increasing angles. We have shown that using such an optimized transducer reduces the occurence of ghost images, and hence performs significantly better in localization experiments.

8. REFERENCES

Bauer, S., Gerhard-Multhaupt, R., and Sessler, G. M. (2004). Ferroelectrets: Soft electroactive foams for transducers. *Physics Today*, february, 37-44.

Peremans, H. (1997). Broad beamwidth ultrasonic transducers for tri-aural perception. *The Journal of the Acoustical Society of America*, **102**, 1567-1572.

Pierce, A. (1994). *Acoustics*. Acoustical Society of America, New York.

Reijniers, J. and Peremans, H. (2004). Towards a theory of how bats navigate through foliage. *Conference proceedings of SAB 2004.*

Schroeder, M. R. and Hall, J. L. (1974). Model for mechanical to neural transduction in the auditory receptor. *J. Acoust. Soc. Am* **55**, 1055-1060.

Slaney, M. (1993). An efficient implementation of the patterson-holdsworth auditory filter bank. *Technical Report* **35**, *Apple Computer Inc.*

Thomas, J., Moss, D., and Vater, M., (Eds.) (2003). *Echolocation in Bats and Dolphins.* University of Chicago Press.